American Mineralogist, Volume 69, pages 1072–1077, 1984

Strain in triclinic alkali feldspars: a crystal structure study

DANA T. GRIFFEN AND BRAD T. JOHNSON[1]

Department of Geology
Brigham Young University
Provo, Utah 84602

Abstract

The crystal structure of a homogeneous unstrained intermediate microcline has been refined to $R = 0.043$ using 2183 reflections ($I > 2\sigma I$) collected with an automated single-crystal X-ray diffractometer. Its composition ($Or_{89}Ab_{11}Cn_1$) and structural state ($t_1o = 0.54$, $t_1m = 0.32$, $t_2o = t_2m = 0.07$) are similar to those of the strained intermediate microcline (coherently exsolved from a cryptoperthitic ternary feldspar) for which the refined structure was reported by Ribbe (1979). A comparison of the two structures has led to a preliminary assessment of the crystallographic effects of strain in terms of bond lengths and bond angles, including a crystallographic explanation of strained lattice parameters.

Relative to corresponding sites in the strained feldspar, $\langle T_1O\text{–}O\rangle$ is larger in the unstrained feldspar by 0.010Å, whereas the T_1m and T_2O sites are the same size, and $\langle T_2m\text{–}O\rangle$ in the unstrained feldspar is slightly smaller. As pointed out by many previous workers, coherent exsolution of the strained feldspar parallel to $(\bar{6}01)$ requires compression of *b* and *c* in the K-rich phase, with a concomitant expansion of *a* predicted by elasticity theory. Our results support these predictions. The strained *a* cell dimension is longer by 0.019Å due to an extension of the double crankshaft chain by rotation of tetrahedra about **c*** and lengthening of the $O_CO\text{–}O_Bm$ and $O_BO\text{–}O_Cm$ tetrahedral edges. These tetrahedral rotations about **c*** and accompanying tilts about *a* result in the shortening of the *b* cell edge in the strained feldspar by 0.046Å. The *c* cell edge of the strained feldspar is shorter by 0.015Å due principally to the smaller size of the T_1O site.

With the exception of compression along *c*, previous predictions that feldspars respond to stress by tilting of tetrahedra rather than by alteration of <T–O> distances, and that the potassium site is a "soft" site, are confirmed. Envisioning tetrahedral tilts in terms of changes in T–O–T angles does not lead to an accurate perception of the geometrical changes that accompany coherent strain.

Introduction

Over the past two decades, strained feldspars have been the subject of a number of studies aimed at elucidating the causes and the crystallographic effects of strain. Smith (1961) and Wright and Stewart (1968) recognized the existence of "anomalous" feldspars with *a* cell dimensions and $(\bar{2}01)$ spacings inconsistently large with respect to *b* and *c*, and explained the anomalous character as strain arising from the coherent or semicoherent intergrowth of potassic and sodic phases. In using Δa as a measure of strain, Stewart and Wright (1974) proposed that a feldspar for which Δa (observed *a* minus *a* predicted from their *b*–*c* plot) exceeded 0.05Å be considered strained. Robin (1974), Tullis (1975), Tullis and Yund (1979), and Yund and Tullis (1983) have considered coherency strain within the framework of elasticity theory in order, among other things, to correct for strain in the unit cell parameters of coherently exsolved monoclinic feldspars. Ribbe (1979) refined the crystal structure of a strained intermediate microcline coherently and cryptoperthitically intergrown with a twinned albitic phase, but because there was no refinement of an unstrained feldspar of similar composition and structural state, he was unable to ascertain the crystallographic effects of strain in terms of individual bond lengths and bond angles.

In examining powder diffraction data for a suite of alkali feldspars collected from the Little Cottonwood Stock near Salt Lake City, Utah, we recognized that these minerals were of nearly the same composition and structural state as Ribbe's strained specimen. Strains ranged from $\Delta a = 0.01$Å to $\Delta a = 0.15$Å, whereas Δa for Ribbe's feldspar was 0.30Å. This suggested the possibility of determining the crystallographic effects of strain by comparing Ribbe's data with the refined structure of one of these feldspars.

[1] Present address: 256 E. Casaloma, Centerville, Utah 84014.

0003–004X/84/1112–1072$02.00

Table 1. Unit cell parameters and strain for *uaf* and *saf*

	uaf	*saf*	*saf - uaf*
a (Å)	8.552(2)	8.643(3)	0.091
b (Å)	12.975(3)	12.929(4)	-0.046
c (Å)	7.205(1)	7.190(3)	-0.015
α (°)	90.09(2)	90.13(3)	0.04
β (°)	115.92(1)	116.24(3)	0.32
γ (°)	89.51(4)	89.60(3)	0.09
V (Å^3)	719.0	720.6	1.6
Δa (Å)	0.01	0.30	

Experimental methods

The crystal chosen came from the groundmass of the porphyritic Little Cottonwood Quartz Monzonite (a granite by the criteria of Streckeisen, 1976) about 20 cm from the intrusive contact with the Big Cottonwood Quartzite. After a series of precession photographs was taken to confirm homogeneity, the crystal, a rough triangular prism ~0.23 mm on each side and 0.15 mm thick, was mounted on a Nicolet P3 automated four-circle single-crystal X-ray diffractometer. Lattice parameters obtained by least squares refinement of 2Θ angles for 30 peaks automatically centered at both +2Θ and −2Θ indicated that the lattice was unstrained. Lattice parameters of our feldspar (*uaf*, *u*nstrained *a*lkali *f*eldspar) and Ribbe's (*saf*, *s*trained *a*lkali *f*eldspar) are compared in Table 1. Intensity scans were run in the Θ–2Θ mode in the range $6° \leq 2\Theta \leq 65°$, at scan rates from 2.0°2Θ/min to 29.3°2Θ/min, depending on diffracted intensity. 2183 symmetrically non-equivalent intensities with $I > 2\sigma I$ were collected with graphite monochromatized Mo$K\alpha$ radiation. Lorentz-polarization corrections were applied, and the structure was refined by least squares methods using the program package SHELX (Sheldrick, 1976), neutral atom scattering factors of Cromer and Mann (1968), and starting positional and thermal parameters from Ribbe (1979). The final *R*-factor, with all atoms anisotropic, was 0.043. Structure factors are listed in Table 2,[2] and refined positional and thermal parameters are shown in Table 3. Table 4 contains a comparison of the bond lengths and bond angles of the unstrained and strained feldspars.

Compositions and structural states

Using the equation of Stewart and Wright (1974), the unit cell volume yielded a composition of $Or_{89}Ab_{11}$ for *uaf*; microprobe analysis gave $Or_{88}Ab_{11}Cn_1$, with Ca and Fe not detected. The composition of *saf* suggested by Ribbe is $Or_{91}Ab_6Cn_3$. Although the compositions are quite close, belaboring their similarity is pointless because neither necessarily represents the composition of the crystals used for structure refinement. That cited by Ribbe is derived from the unit cell volume of the K-rich phase in the crystal used for structure refinement, assuming the same Or/Cn ratio as that of the bulk composition given by MacKenzie and Smith (1962, who obtained it from Upton, 1960). The composition we give for *uaf* was obtained from fragments of the same groundmass crystal as the fragment used for structure refinement, but we observed slight compositional inhomogeneity ($\pm Or_1$, $\pm Ab_1$), and $Or_{88}Ab_{11}Cn_1$ is the average. (The composition $Or_{89}Ab_{11}$ for *uaf* was obtained from the cell volume of the crystal used for structure refinement.) The celsian component makes *saf* slightly more aluminous than *uaf*, and, of course, requires partial substitution of barium for potassium; but Ba and K are about the same size, and the additional Al amounts to only 0.02 atoms. It can thus justifiably be argued that the comparison contemplated is reasonable.

The structural state of *uaf* was estimated in three ways, and the results are shown in Table 5, with results for *saf* as well. Using the *b*–*c* and α^*-γ^* plots of Stewart and Wright (1974), tetrahedral topochemistries were obtained that are very similar to those of *saf* determined by the same method. Using the method of Ribbe (1975) and the mean bond lengths obtained from our structure refinement, we obtain essentially the same structural state for *uaf*, whereas the apparent structural state for *saf* is somewhat less ordered. Kroll (1980) provided diagrams for the determination of structural state based on the [110] and [1$\bar{1}$0] translation distances, and the results of this method are also shown in Table 5. We note that for method 2, total Al values were constrained computationally to 1.01 and 1.03 atoms, respectively, consistent with the reported compositions, and resulting in slightly higher values than calculated by Ribbe (1979). For methods 1 and 3, no attempt was made to correct for the "excess" Al contributed by the Cn component.

Because the structural state of *saf* cannot be unequivocally determined from the data available, we are not able to say which method gives the truest estimate. The most divergent structural states for *uaf* and *saf* are yielded by the method of Ribbe (1975), which uses observed bond lengths in the calculation. We suggest below that there is good reason to believe that at least some of the bond lengths in T_1O, and perhaps in T_2m, are "strained". On the other hand, *b* and *c* in *saf* are both smaller than in a corresponding unstrained feldspar, and it is not known whether these differences compensate to yield correct structural states on the diagrams of Stewart and Wright (1974) and Kroll (1980). It can be said only that the structural states of our specimen and Ribbe's are close enough to justify comparison of the structures at the "first approximation" level.

Discussion

Potassium site

Using reasonable guesses for the radii of K, Na, and Ba in a feldspar (for example, the nine-coordinated radii of

[2] To receive a copy of Table 2, order Document AM-84-255 from the Business Office, Mineralogical Society of America, 2000 Florida Avenue, N.W., Washington, D.C. 20009. Please remit $5.00 in advance for the microfiche.

Table 3. Fractional coordinates and temperature factor coefficients for *uaf*

Atom	*x*	*y*	*z*	u_{11}	u_{22}	u_{33}	u_{12}	u_{13}	u_{23}
K	0.2838(1)	0.9985(1)	0.1366(1)	0.0189(3)	0.0254(3)	0.0214(3)	0.0000(2)	0.0058(2)	-0.0001(2)
T_1O	0.0096(1)	0.1850(1)	0.2229(1)	0.0220(4)	0.0149(3)	0.0135(3)	-0.0032(3)	0.0083(3)	-0.0015(2)
T_1m	0.0093(1)	0.8165(1)	0.2260(1)	0.0211(3)	0.0139(3)	0.0131(3)	0.0018(2)	010083(3)	0.0018(2)
T_2O	0.7086(1)	0.1183(1)	0.3434(1)	0.0191(3)	0.0105(3)	0.0127(3)	-0.0005(2)	0.0068(2)	0.0003(2)
T_2m	0.7074(1)	0.8829(1)	0.3459(1)	0.0191(3)	0.0105(3)	0.0131(3)	-0.0009(2)	0.0068(3)	0.0000(2)
O_A1	0.9999(3)	0.1442(2)	0.9959(3)	0.0325(11)	0.0176(9)	0.0231(10)	0.0004(8)	0.0128(8)	0.0007(7)
O_A2	0.6352(3)	0.0012(2)	0.2851(3)	0.0285(10)	0.0130(8)	0.0214(10)	-0.0008(7)	0.0048(8)	0.0003(7)
O_BO	0.8255(3)	0.1453(2)	0.2263(4)	0.0295(11)	0.0323(12)	0.0264(11)	-0.0036(9)	0.0182(9)	0.0014(9)
O_Bm	0.8273(3)	0.8552(2)	).2301(4)	0.0303(11)	0.0322(12)	0.0288(11)	0.0036(9)	0.0186(9)	0.0001(9)
O_CO	0.0344(3)	0.3129(2)	0.2579(3)	0.0248(10)	0.0185(9)	0.0229(10)	-0.0032(7)	0.0088(8)	-0.0032(7)
O_Cm	0.0353(3)	0.6902(2)	0.2616(3)	0.0252(10)	0.0198(9)	0.0230(10)	0.0027(8)	0.0099(8)	0.0044(7)
O_DO	0.1842(3)	0.1251(2)	0.4064(3)	0.0291(11)	0.0207(9)	0.0126(8)	0.0004(8)	0.0042(8)	0.0014(7)
O_Dm	0.1809(3)	0.8741(2)	0.4077(3)	0.0283(10)	0.0200(9)	0.0131(8)	-0.0020(8)	0.0037(8)	-0.0011(7)

esd's, shown in parentheses, refer to the last decimal place.

u_{ij} are coefficients in the expression $\exp[-2\pi^2(a^{*2}u_{11}h^2 + b^{*2}u_{22}k^2 + c^{*2}u_{33}\ell^2 + 2a^*b^*u_{12}hk + 2a^*c^*u_{13}h\ell + 2b^*c^*u_{23}k\ell)]$.

Whittaker and Muntus (1970), or those published in 1976 by Shannon), one predicts, within reasonable estimates of error, the observed difference in mean bond lengths for the K polyhedra. Figure 1 displays the K-site with differences in individual bond lengths shown. It is obvious that neither an isotropic dilation nor a shift in position of the cation can account for the observed differences in bond lengths. The geometrical differences in the potassium sites of *uaf* and *saf* must be attributed to anisotropic dilations and/or rotations of the tetrahedral framework. Nonetheless, it is apparent that the K-site is a "soft" site, as predicted by Hazen and Finger (1979).

Tetrahedral sites

The maximum observed difference in mean tetrahedral bond lengths occurs at the T_1O site, where it is 0.010Å. This difference is not statistically convincing in itself, but is probably real inasmuch as it arises from fairly substantial differences in both T_1O–O_A1 and T_1O–O_CO, and in four of the six tetrahedral edge lengths (see Table 4). (That is, it is due not to uniformly small and insignificant differences, but to a few significant ones.) A difference of 0.010Å is more, by as much as a factor of 3, than would be expected from the slight difference in structural states between *uaf* and *saf*, according to columns 1 or 3 of Table 5. (If column 2 is used, then the observed size difference is predicted, naturally, because column 2 is based on mean bond lengths.) Even if the dissimilarity in mean size is attributed to composition alone, the variation in corresponding individual bond lengths must be considered a strain-generated distortion. Further evidence that the T_1O site undergoes significant compression as a result of strain will be presented below in the section on lattice parameters. T_1m and T_2O possess virtually identical geometries in the two feldspars. Mean bond lengths for the T_2m sites differ by only 0.005Å, but two factors suggest that this small difference may also be real. First, the difference is largely attributable to the T_2m–O_CO distance, which is longer in *saf* by 0.012Å, compensating for the 0.014Å shorter T_1O–O_CO distance; second, two T_2m edge lengths are substantially longer in *saf* than in *uaf*.

Lattice parameters

It is well known that K-rich feldspars which are elastically strained due to coherency with an Na-rich phase on ~(601) have larger *a* cell edges, and smaller *b* and *c* cell edges, than unstrained feldspars of the same compositions and structural states. This is because the *b* and *c* cell dimensions of the K-rich and Na-rich phases must match across lamellar interfaces, and, in the K-rich phase, *a* expands as an elastic response to compression of *b* and *c* (Tullis, 1975). For the two feldspars in question here, the differences in the *a*, *b*, and *c* cell edges (Table 1) are in the ratio 6:−3:−1.

b cell dimension. Figure 2 shows a chain of six tetrahedra that constitute a repeat in the *b* direction, projected onto (001). Numbers along tetrahedral edges are differences in Ångstroms (*saf* minus *uaf*). Numbers at the top of the figure between vertical lines are the projections of the edge-length differences onto the *b*-axis. Curved arrows represent rotations of tetrahedra about **c*** in *saf* relative to *uaf*. Finally plusses (+) indicate positive (out-of-page) deviations of tetrahedral corners in *saf* relative

Table 4. Interatomic distances (Å) and angles (°) in *uaf* and *saf*

	T-O distances			O-O distances		O-T-O angles	
	uaf	*saf*		*uaf*	*saf*	*uaf*	*saf*
T_1O tetrahedron							
$T_1O - O_A1$	1.685	1.667	$O_A1 - O_BO$	2.674	2.662	105.6	105.9
$- O_BO$	1.672	1.668	$- O_CO$	2.820	2.788	113.8	113.6
$- O_CO$	1.680	1.666	$- O_DO$	2.686	2.668	105.7	105.6
$- O_DO$	1.685	1.682	$O_BO - O_CO$	2.772	2.751	111.6	111.2
			$- O_DO$	2.770	2.777	111.2	112.0
			$O_CO - O_DO$	2.736	2.717	108.8	108.5
Mean	1.681	1.671		2.743	2.726	109.5	109.5
T_1m tetrahedron							
$T_1m - O_A1$	1.647	1.647	$O_A1 - O_Bm$	2.634	2.635	106.3	106.5
$- O_Bm$	1.644	1.642	$- O_Cm$	2.767	2.759	113.8	113.3
$- O_Cm$	1.657	1.655	$- O_Dm$	2.641	2.644	105.9	106.1
$- O_Dm$	1.662	1.661	$O_Bm - O_Cm$	2.717	2.714	110.8	110.8
			$- O_Dm$	2.733	2.739	111.5	112.1
			$O_Cm - O_Dm$	2.692	2.683	108.4	108.0
Mean	1.653	1.651		2.697	2.696	109.5	109.5
T_2O tetrahedron							
$T_2O - O_A2$	1.632	1.624	$O_A2 - O_BO$	2.642	2.643	109.4	109.5
$- O_BO$	1.606	1.612	$- O_Cm$	2.572	2.569	104.5	104.4
$- O_Cm$	1.622	1.627	$- O_Dm$	2.642	2.635	108.5	108.4
$- O_Dm$	1.624	1.624	$O_BO - O_Cm$	2.663	2.669	111.2	110.9
			$- O_Dm$	2.673	2.683	111.7	112.0
			$O_Cm - O_Dm$	2.680	2.684	111.3	111.3
Mean	1.621	1.622		2.645	2.647	109.4	109.4
T_2m tetrahedron							
$T_2m - O_A2$	1.636	1.639	$O_A2 - O_Bm$	2.638	2.646	108.3	108.5
$- O_Bm$	1.618	1.622	$- O_CO$	2.576	2.592	104.7	104.9
$- O_CO$	1.618	1.630	$- O_DO$	2.641	2.640	108.7	108.4
$- O_DO$	1.615	1.616	$O_Bm - O_CO$	2.660	2.680	110.6	111.0
			$- O_DO$	2.675	2.677	111.7	111.5
			$O_CO - O_DO$	2.688	2.692	112.5	112.1
Mean	1.622	1.627		2.646	2.655	109.4	109.4
K polyhedron			T-O-T angles				
$K - O_A2$	2.714	2.746	$T_1O-O_A1-T_1m$			143.7	144.8
$- O_A1$	2.876	2.900	$T_2O-O_A2-T_2m$			138.3	138.3
$- O_A1$	2.876	2.902	$T_1O-O_BO-T_2O$			152.3	151.7
$- O_DO$	2.935	2.942	$T_1m-O_Bm-T_2m$			153.1	153.0
$- O_Dm$	2.955	2.958	$T_1O-O_CO-T_2m$			130.9	131.6
$- O_BO$	3.012	3.014	$T_1m-O_Cm-T_2O$			131.1	131.7
$- O_Bm$	3.046	3.053	$T_1O-O_DO-T_2m$			141.1	141.1
$- O_CO$	3.072	3.089	$T_1m-O_Dm-T_2O$			141.8	141.8
$- O_Cm$	3.165	3.165					
Mean	2.961	2.974				141.5	141.8

esd's - uaf: T-O and K-O, 0.002; O-O, 0.003; angles, 0.1
saf: T-O and K-O, 0.005; O-O, 0.007; angles, 0.3

Table 5. Estimates of structural states of *uaf* and *saf*

Method:	1		2		3	
Reference:	Stewart & Wright (1974)		Ribbe (1975)		Kroll (1980)	
	uaf	*saf*	*uaf*	*saf*	*uaf*	*saf*
t_1O	0.54	0.52	0.54	0.48	0.54	0.50
t_1m	0.32	0.34	0.32_5	0.33	0.32	0.33
t_2O	0.07	0.07	0.07_3	0.11	0.07	0.08_5
t_2m	0.07	0.07	0.07_3	0.11	0.07	0.08_5

to *uaf*, and relative to O_A2 in both feldspars (labelled "0" for zero relative deviation out-of-page).

The sum of the edge-length differences is −0.002Å, indicating that the contraction of the *b* cell edge in *saf* is not due to size differences in tetrahedra. (The sum of the *projected* differences is, of course, −0.046Å, the difference in *b* cell dimensions between *saf* and *uaf*.) Thus the contraction of *b* in the strained feldspar is accomplished by rotations of tetrahedra about **c*** (curved arrows in Fig. 2) caused by extension of the double crankshaft chain (see below), along with slight rotations about *a* (+'s and 0's in Figure 2).

c cell dimension. The 4-membered ring of tetrahedra in Figure 3 defines a repeat in the *c* direction. As before, numbers representing differences (*saf* minus *uaf*) in relevant angles and distances are shown. The symbols <90 and >90 in the inside corners of the ring indicate absolute magnitudes of the O–O–O angles in both *saf* and *uaf*. Note that the *c* cell dimension consists of the heights of two triangular faces (both essentially in the (010) plane) plus the distance across the inside of the 4-membered ring.

Taking the distance across the ring to be the average of the two parallel sides, the sum of the three relevant distances (−0.012Å) accounts for 80% of the observed difference in the two *c* dimensions. The four bridging oxygens at the corners of the ring are not coplanar, and further out-of-plane torsion accounts for the other 20%. Note, however, that the only distance that is negative is the height of the face of the T_1O tetrahedron. Thus, the compression of T_1O in the strained feldspar results in nearly all of the observed shortening of the *c* lattice parameter, and tends to confirm, as suggested above, that

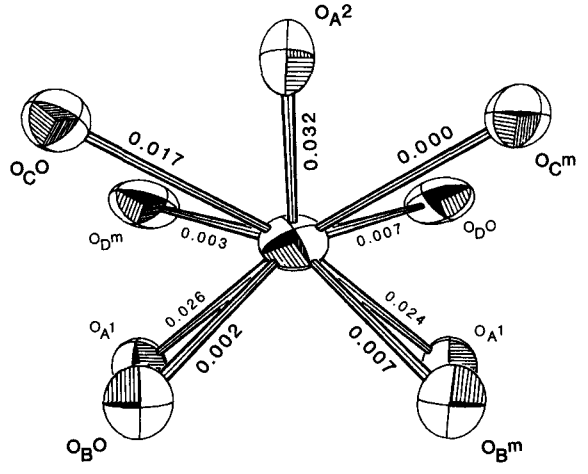

Fig. 1. K-sites in a triclinic alkali feldspar. Numerical labels are differences between bond lengths in *saf* and *uaf* (strained minus unstrained). Drawing was made with ORTEP (Johnson, 1976).

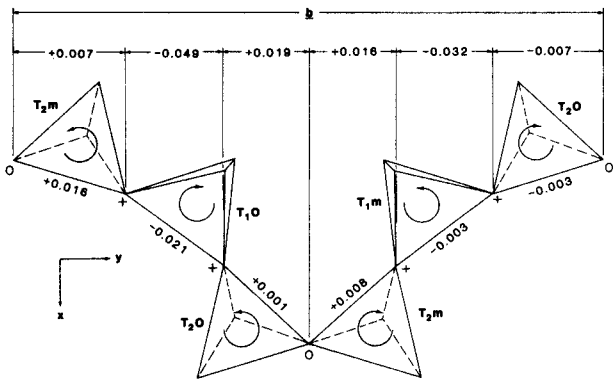

Fig. 2. A portion of the alkali feldspar structure projected onto (001), showing a repeat in the *b* direction. See text for explanation of labels.

the compression is partly strain-generated and not solely compositional.

a cell dimension. The way in which expansion of *a* is accomplished can be seen by referring to Figure 4. This depicts the *a* repeat along one side of the feldspar double crankshaft chain, projected onto (001). The labels on tetrahedral edges and intertetrahedral angles are differences, *saf* minus *uaf*. Note that all of the angular differences are positive, indicating an angular extension of the chain in the strained feldspar. Moreover, the two tetrahedral edges that are most nearly parallel to *a* are the two that are longer in *saf*. Thus the *a* cell edge of the strained mineral extends by "stretching" of the double crankshaft chain and favorable orientation of the longer tetrahedral edges.

Coherency strain and elastic properties

Hazen and Finger (1979) have attributed the small bulk

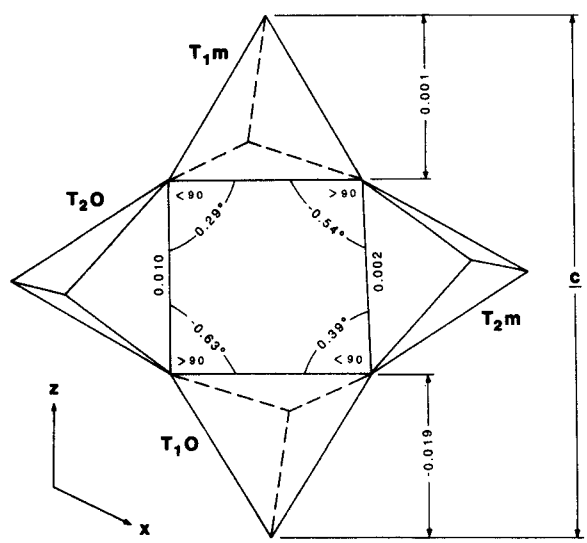

Fig. 3. A 4-membered ring of tetrahedra that defines a repeat in the *c* direction, projected onto (010). Numerical labels are discussed in the text.

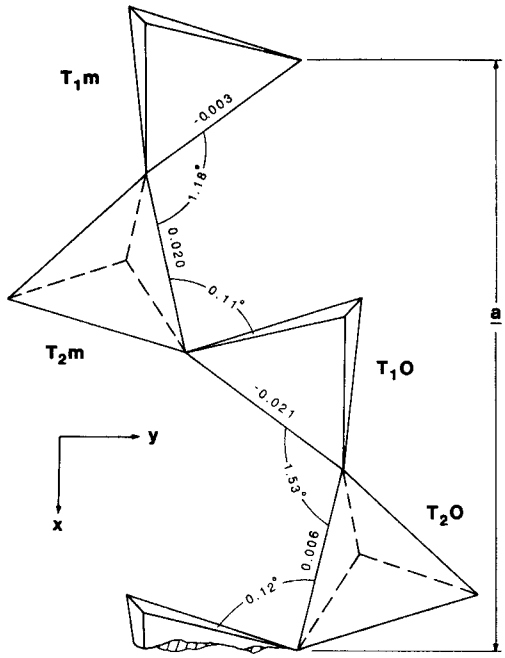

Fig. 4. An *a* cell edge repeat along one side of the double crankshaft chain, projected onto (001). Numerical labels are explained in the text.

moduli of framework silicates to the freedom of the corner-linked tetrahedra to tilt despite the relative incompressibility of the tetrahedra themselves. Our comparison of *uaf* and *saf* confirms that the adjustments in *a* and *b* required by coherency are largely accomplished by tilting of tetrahedra. Tetrahedral tilting appears to be a secondary mechanism for compression of *c*, however.

While these authors have envisioned tilting of tetrahedra as "metal–oxygen–metal bond bending or oxygen–oxygen compression", our results suggest that this is an oversimplification. The data in Table 4 and Figures 2, 3, and 4 show that there are variations in tetrahedral O–O distances, but these variations cannot, of themselves, account for any of the three cell edge differences. There are also differences in T–O–T angles, but, on the average, these are less than the differences in intertetrahedral tilt angles. Along the stretched double crankshaft chain parallel to *a*, for example, the mean absolute difference in intertetrahedral angles is ~0.7°, while the mean absolute difference in the associated T–O–T angles is ~0.4°. Moreover, comparison of the T–O bond lengths shows that, for all but the T_1m site, each Al/Si atom has moved relatively away from the tetrahedral edge labelled in Figure 4, and the cation at T_1m has remained in the same relative position. These shifts have resulted in two of the T–O–T angles decreasing while the other two increased, even though all of the intertetrahedral angles increased. Evidently, the variations in T–O–T angles do not always provide adequate descriptions of the framework distortions of which bulk moduli are a reflection.

Conclusion

It has been long known that coherent intergrowth of alkali feldspars parallel to ~(601) results in shortening of *b* and *c* and expansion of *a* in the K-rich lamellae, and that these unit cell distortions are due to elastic response of the lamellae to coherency stress. The way in which the distortions are accomplished, at the atomic level, has not been known. Refinement of the crystal structure of an unstrained alkali feldspar of similar composition and structural state to Ribbe's (1979) strained alkali feldspar has provided some insight into the crystallographic effects of strain.

Generalizations drawn from the present work must be considered somewhat tentative for three reasons. First, the two feldspars discussed, while similar in composition, are probably not identical; second, available evidence points to nearly equivalent structural states, but this cannot be unequivocally confirmed; and third, the influence of composition on the strain effects, at the atomic level, is unknown, so conclusions made here might not be fully applicable to strained feldspars of other compositions. Nonetheless, the following conclusions appear reasonable:

(1) Compression of the *b* cell in K-rich feldspars that are strained due to coherency on ~(601) is accomplished mainly by rotation of tetrahedra about ~**c***.

(2) Compression of *c* occurs principally by a strain-induced volume change at the T_1O site

(3) The same tetrahedral rotations about ~**c*** that shorten *b* lengthen *a*, by angular extensions of the double crankshaft chain.

(4) The predictions of Hazen and Finger (1979) that lattice parameter changes in feldspars subjected to stress are accomplished by tilting of tetrahedra and that the potassium site is a "soft" site are confirmed, except for compression of the *c* cell edge.

(5) Tetrahedral tilts are not always mimicked by changes in T–O–T angles, and, in the structures compared here, the former provide a better description of framework distortion. With Taylor (1983), we see the crystallographic response of a feldspar to any stress, including coherency, as a dynamic one, in which atoms adjust to equilibrium positions, with resultant changes in T–O bond lengths, tetrahedral shapes, and framework geometry.

Acknowledgments

We thank W. P. Nash for the use of the electron microprobe at the Department of Geology and Geophysics, University of Utah, and David Filar for technical assistance on that instrument. The College of Physical and Mathematical Sciences at BYU generously provided computer time. A helpful review by Jan A. Tullis resulted in substantial improvement of the manuscript.

References

Cromer, D. T. and Mann, J. B. (1968) X-ray scattering factors computed from numerical Hartree–Fock wave functions. Acta Crystallographica, A24, 321–324.

Hazen, R. M. and Finger, L. W. (1979) Bulk modulus–volume relationship for cation–anion polyhedra. Journal of Geophysical Research, 84, 6723–6728.

Johnson, C. K. (1976) OR TEP-II: A FORTRAN thermal-ellipsoid plot program for crystal structure illustrations. U. S. National Technical Information Service, ORNL-5138.

Kroll, Herbert (1980) Estimation of the Al,Si distribution of alkali feldspars from lattice translations tr[110] and tr[1$\bar{1}$0]. Revised diagrams. Neues Jahrbuch für Mineralogie Monatshefte, 31–36.

MacKenzie, W. S. and Smith, J. V. (1962) Single crystal x-ray studies of crypto- and microperthites. Norsk Geologisk Tiddskrift, 42/2, 72–103.

Ribbe, P. H. (1975) The chemistry, structure, and nomenclature of feldspars. In P. H. Ribbe, Ed., Feldspar Mineralogy, p. R-1–R-22. Mineralogical Society of America, Washington, D.C.

Ribbe, P. H. (1979) The structure of a strained intermediate microcline in cryptoperthitic association with twinned plagioclase. American Mineralogist, 64, 402–408.

Robin, P.-Y. F. (1974) Stress and strain in cryptoperthite lamellae and the coherent solvus of alkali feldspars. American Mineralogist, 59, 1299–1318.

Shannon, R. D. (1976) Revised effective ionic radii and systematic studies of interatomic distances in halides and chalcogenides. Acta Crystallographica, A32, 751–767.

Sheldrick, G. M. (1976) SHELX-76: a programme for crystal structure determination, University of Cambridge.

Smith, J. V. (1961) Explanation of strain and orientation effects in perthites. American Mineralogist, 46, 1489–1493.

Stewart, D. B. and Wright, T. L. (1974) Al/Si order and symmetry of natural alkali feldspars, and the relationship of strained cell parameters to bulk composition. Bulletin de la Société francaise de Minéralogie et de Cristallographie, 97, 356–377.

Streckeisen, A. (1976) To each plutonic rock its proper name. Earth-Science Reviews, 12, 1–33.

Taylor, D. (1983) The structural behaviour of tetrahedral framework compounds—a review. Part I. Structural behaviour. Mineralogical Magazine, 47, 319–326.

Tullis, Jan (1975) Elastic strain effects in coherent perthitic feldspars. Contributions to Mineralogy and Petrology, 49, 83–91.

Tullis, Jan and Yund, R. A. (1979) Calculation of coherent solvi for alkali feldspar, iron-free clinopyroxene, nepheline–kalsilite, and hematite–ilmenite. American Mineralogist, 64, 1063–1074.

Upton, B. G. J. (1960) The alkaline igneous complex of Kungnat Fjeld, South Greenland. Meddelelser om Grønland, 123, 1–145.

Whittaker, E. J. W. and Muntus, R. (1970) Ionic radii for use in geochemistry. Geochimica et Cosmochimica Acta, 34, 945–956.

Wright, T. L. and Stewart, D. B. (1968) X-ray and optical study of alkali feldspar: I. Determination of composition and structural state from refined unit cell parameters and 2*V*. American Mineralogist, 53, 38–87.

Yund, R. A. and Tullis, Jan (1983) Strained cell parameters for coherent lamellae in alkali feldspars and iron-free pyroxenes. Neues Jahrbuch für Mineralogie Monatshefte, 1983, 22–34.

Manuscript received, September 22, 1983;
accepted for publication, June 20, 1984.